Conformational properties of blends of cyclic and linear polymer melts

Gopinath Subramanian[1] and Sachin Shanbhag[1,2,*]

[1]*School of Computational Science, Florida State University, Tallahassee, Florida 32306, USA*

[2]*Department of Chemical and Biomedical Engineering, FAMU-FSU College of Engineering, Tallahassee, Florida 32310-6046, USA*

(Received 18 September 2007; revised manuscript received 15 November 2007; published 14 January 2008)

An adapted version of the annealing algorithm to identify primitive paths of a melt of ring polymers is presented. This algorithm ensures that the primitive path length becomes zero for nonconcatenated rings, and that no entanglements are observed. The bond-fluctuation model was used to simulate ring-linear blends with $N=150$ and 300 monomers. The primitive path length and the average number of entanglements of the linear component were found to be independent of the blend composition. In contrast, the primitive path length and the average number of entanglements on a ring molecule increased approximately linearly with the fraction of linear chains, and for large N, they approached values comparable with linear chains. Threading of ring molecules by linear chains, and ring-ring interactions were observed only in the presence of linear chains. It is conjectured that for large N, these latter interactions facilitate the formation of a percolating entangled network, thereby resulting in a disproportionate retardation of the dynamical processes.

DOI: 10.1103/PhysRevE.77.011801 PACS number(s): 83.80.Tc, 02.70.Uu

I. INTRODUCTION

Ring polymers are scientifically fascinating because they lack chain ends. Chain ends enable other polymer architectures, such as linear chains to "reptate," and branched polymers to "retract," and thereby renew their configurations. In the tube model for entangled polymers, the connection between relaxation and diffusion properties, and the underlying molecular picture of a test chain immersed in a sea of obstacles, is established by solving a one-dimensional diffusion problem that describes the motion of chain ends in a hypothetical tube [1–3]. Concentrated solutions, or melts, of cyclic polymers force us to reexamine this connection. Theoretical studies [4–7] have considered the motion of a cyclic polymer in a gel, and it has been suggested that ring polymers thrust and pull on unentangled loops, executing amoebalike motion. There is also a substantial body of viscoelastic experimental data on polystyrene and polybutadiene rings [8–11] comparing the properties of linear and cyclic polymers. Recent advances in alternative synthetic routes [12] to synthesize polyethylene rings are highly encouraging, especially since polyethylene has a low entanglement molecular weight. Numerous computational studies of ring polymers [13–20] have explored the conformational properties of ring polymers quite extensively.

However, blends of rings and linear chains have not been studied extensively, and thus, only a small body of literature exists on the subject [21,22]. Blend systems are important because most experimental data on "pure rings" are in fact data on ring-linear blends due to contamination, or limitations of purification methods. The dynamics of such ring-linear blends are extremely sensitive to the concentration of linear chains. It was demonstrated that the zero-shear viscosity η_0 of polystyrene rings, intentionally contaminated with narrow fractions of linear chains, varied sharply with the concentration of the rings c_R according to $\eta_0 \propto c_R^{-5.6}$ [23]. More recently, it was reported that the terminal relaxation time of a polystyrene ring-linear blend (both components having molecular weight 200 KDa) with 5% by volume of the linear component is greater than the relaxation time of the linear chain itself [24]. Furthermore, studies using fluorescence microscopy to track entangled solutions of linear and cyclic DNA highlight the prominent role that topology plays in the dynamics of ring-linear blends [25,26]. Here, for 45-kbp DNA at 1 mg/ml concentration, the diffusivity of a tracer ring polymer dropped by two orders of magnitude when the surrounding matrix of ring polymers was replaced with linear chains.

As a preliminary step toward understanding the unexpected sensitivity of the dynamics of ring-linear systems, this paper examines the topological properties of blends of linear and ring polymers using the bond-fluctuation model (BFM). Further, a recently developed algorithm to obtain primitive paths (PP) of linear chains is extended to analyze ring and ring-linear polymers.

II. MODEL AND METHODS

Shaffer's version of the BFM (S-BFM) was used in this work. It has been used to model linear [27,28], star [29], and ring polymers [13]. This method has recently been extended to blends of ring and linear polymers [22]. In S-BFM, monomers or beads are placed on a simple cubic lattice. The initialization method described in previous papers was modified to generate an equilibrated blend of ring and linear molecules. This modified method has been described in detail elsewhere [22], and hence will only be summarized here.

A. Equilibration

N_{pR} nonconcatenated rings, each consisting of N_R monomers, and N_{pL} linear chains, each consisting of N_L monomers were embedded in a three-dimensional cubic lattice in a simulation box of size $L \times L \times L$. Throughout this paper, length is expressed in units of lattice spacing. To simulate

*sachins@scs.fsu.edu

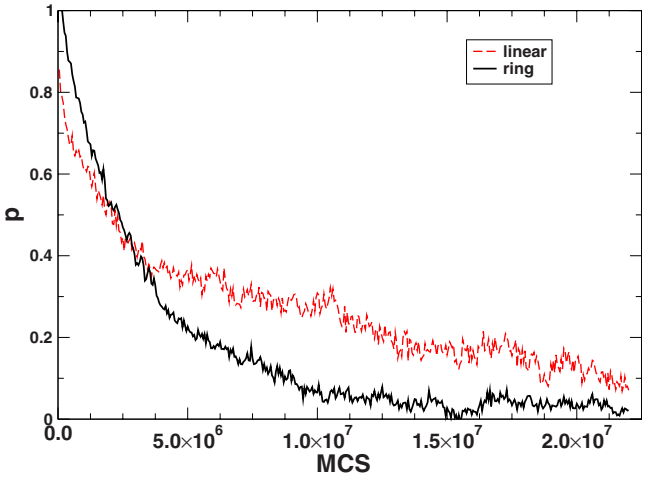

FIG. 1. (Color online) Autocorrelation of the end-to-end vectors of linear polymers for $N_L=300$, and the diametrical vector of ring polymers for $N_R=300$. The fraction of linear chains $\phi_L/\phi=0.5$. Autocorrelation of the diametrical vector of ring polymers $p_R(t)$ decays faster than the autocorrelation of the end-to-end vector of the linear chains $p_L(t)$.

meltlike behavior, the total fractional occupancy of the lattice was maintained at $\phi=\phi_R+\phi_L=0.5$, where ϕ_R and ϕ_L represent the fractional occupancy of ring and linear molecules, respectively. A value of $\phi=0.5$ is adequate to describe the behavior of well-entangled polymers [27]. During equilibration, a trial move is attempted by displacing a randomly selected bead, belonging to either a ring or linear chain, by one lattice unit. It is accepted if it does not violate the excluded volume, chain connectivity, and chain uncrossability constraints.

For linears, the autocorrelation of the end-to-end vector $p_L(t)=\langle \mathbf{R}(t)\cdot\mathbf{R}(0)\rangle/\langle R^2(0)\rangle$ was monitored. Here, $\mathbf{R}(t)=\mathbf{r}_{N_L}(t)-\mathbf{r}_1(t)$ is the vector connecting the positions of beads 1 and N_L at time t, and $\langle\cdots\rangle$ is an average over all chains of a particular topology in the system. Similarly, for rings, the decay of the autocorrelation $p_R(t)$ of the diametrical vector connecting beads 1 and $N_R/2$, $\mathbf{r}_{N_R/2}(t)-\mathbf{r}_1(t)$ was monitored. The system was assumed to be equilibrated when both p_L and p_R had dropped below 0.1 (see Fig. 1 and refer to the appendix for further information regarding equilibration).

The annealing algorithm for S-BFM [30] has been adapted and further developed to examine the PP network [28]. This new algorithm helps to identify the structure of the underlying primitive path network [31,32]. A simple geometrical algorithm to locate the positions of entanglement points was constructed and was subsequently labeled as the "identification of local deviations" (ILD) algorithm [33,34].

B. Primitive path network

In the annealing algorithm, the end beads of all the equilibrated linears are held fixed while the interior beads are free to move. The intramolecular excluded volume constraint is turned off while the intermolecular excluded volume constraint is enforced. This is done to facilitate the shrinkage of the chain contours while maintaining their noncrossability with other chains. In the lattice model [28], the probability with which moves that increase the PP length are accepted is decreased according to the expression

$$p_{\mathrm{acc}}(t)=\min\left\{1,\exp\left[-A\Delta L\left(\frac{t}{\tau_{\mathrm{anneal}}}\right)^2\right]\right\}, \qquad (1)$$

where ΔL is the change in contour length (positive or negative) due to a trial move, and τ_{anneal} is the duration of the annealing process. In earlier simulations [28,34], the constants were set as $A=16$ and $\tau_{\mathrm{anneal}}\approx 10\tau_{\mathrm{Rouse}}$, where τ_{Rouse} is the Rouse relaxation time. This choice implied that $p_{\mathrm{acc}}=1/e$ when $t/\tau_{\mathrm{anneal}}=1/4$ for $\Delta L=+1$. However, it was recently argued [32] that these choices were too conservative. In the present study $A=16$ was maintained, but τ_{anneal} was changed to $10\tau_e$, where $\tau_e\approx 5000$ MCS is the Rouse time corresponding to an entanglement segment [33,35].

Lattice and off-lattice annealing methods, as well as other geometrical algorithms [36,37] were originally conceived for a system comprising monodisperse linear chains. They may be extended to star and other branched structures, in which chain ends are affixed as in linear molecules. However, as described later, an important modification had to be introduced for cyclic polymers.

C. Identification of local deviations

It was proposed that the "local" structure of the PP needs to be examined to identify the spatial location of individual entanglements in S-BFM. If the length of any small segment of the PP deviates from the shortest possible path connecting its ends, the presence of a topological constraint in that neighborhood which prevents the PP segment from decreasing its length may be indirectly inferred. It was argued that the smallest such element which could be examined was one containing three consecutive PP monomers, or two consecutive bonds. Thus, it was hypothesized that if the trajectory of the PP between a bead and its second-nearest neighbor does not follow the shortest possible path along the cubic lattice, it is due to an obstacle or entanglement. It was shown that this natural choice led to good agreement with the number of entanglements Z calculated from ensemble averages of monodisperse linear chains. A detailed description of this argument and simulations supporting it are available elsewhere [34].

III. RESULTS

The present work studied the properties of two series of ring-linear blends with degree of polymerization $N=150$ and 300. In each series, the degree of polymerization of the ring and linear molecules were identical, i.e., $N_R=N_L=N$ at a total fractional occupancy $\phi=\phi_R+\phi_L=0.5$. The composition of the ring-linear blend was varied from $\phi_R=0.5$ (pure rings) to $\phi_R=0.0$ (pure linears). Table I summarizes the details of the systems studied.

A. Size

In melts, ring polymers assume more compact conformations when compared with linear chains having the same

TABLE I. Description of the systems simulated. Simulation box size $L_{box}=60$, and total density $\phi_R+\phi_L=0.5$.

ϕ_L	ϕ_R	N_{pL}	N_{pR}	R_{gL} [a]	R_{gR} [a]
			$N=150$		
0.500	0.000	720	0	7.95±0.10	
0.479	0.021	690	30	8.21±0.07	5.85±0.16
0.458	0.042	660	60	8.10±0.07	5.82±0.11
0.438	0.063	630	90	8.19±0.08	5.76±0.10
0.375	0.125	540	180	7.99±0.08	5.80±0.07
0.313	0.188	450	270	8.02±0.09	5.50±0.05
0.250	0.250	360	360	8.21±0.10	5.54±0.05
0.188	0.313	270	450	8.16±0.12	5.46±0.04
0.125	0.375	180	540	8.15±0.15	5.30±0.03
0.063	0.438	90	630	8.01±0.18	5.25±0.03
0.042	0.458	60	660	8.04±0.25	5.25±0.03
0.021	0.479	30	690	8.33±0.34	5.16±0.03
0.000	0.500	0	720		5.09±0.14
			$N=300$		
0.500	0.000	360	0	11.20±0.17	
0.450	0.050	324	36	11.32±0.15	8.60±0.20
0.375	0.125	270	90	11.51±0.18	8.71±0.20
0.250	0.250	180	180	12.27±0.25	8.10±0.11
0.167	0.333	120	240	12.02±0.29	7.50±0.11
0.100	0.400	72	288	12.37±0.33	7.24±0.08
0.050	0.450	36	324	12.35±0.55	7.10±0.07
0.025	0.475	18	342	11.67±0.56	6.96±0.05
0.000	0.500	0	360		7.02±0.06

[a] R_g data was presented originally in [22].

degree of polymerization, i.e., $R_{gR}\sim N_R^{\nu}$ with $\nu\approx 0.4$, where R_{gR} is the radius of gyration of the rings. Upon gradually substituting some of the ring polymers with linear chains, the remaining ring molecules swell. In the limit of infinite dilution, their size scales as $R_{gR}\sim N_R^{0.5}$.

Recently, a scaling argument based on the blob model was presented [22], and shown to capture this transition. Ring-linear blends were modeled as a semidilute solution of ring polymers in a Θ solvent consisting of linear chains. The model predicted that the size of the ring polymer remained unchanged up to an overlap concentration ϕ_R^*. Beyond ϕ_R^* the size of the ring decreased according to $R_{gR}\sim \phi_R^{-1/5}$.

These predictions were tested by performing Monte Carlo simulations of ring-linear blends using the BFM for the systems mentioned in Table I. The results of the simulation validated the scaling model. As predicted by the scaling model, size of the linears R_{gL} was independent of the concentration of rings ϕ_R, and was approximately equal to the size of a coil in a pure linear melt, where $R_{gL}(\phi_R=0)=7.95\pm0.10$ and 11.20 ± 0.17 for $N=150$ and 300, respectively.

The radius of gyration of ring polymers, however, increased with the fraction of linear chains in the melt. For $N=150$, R_{gR} increased from 5.18 ± 0.03 (pure rings) to 5.85 ± 0.17 when $\phi_L=0.48$. For $N=300$, R_{gR} increased from 7.02 ± 0.06 (pure rings) to 8.60 ± 0.20 when $\phi_L=0.45$. Thus, it may be concluded that as ϕ_L increases, linear chains infiltrate the volume occupied by the rings and force them to swell. The average volume of a ring R_{gR}^3 increased by approximately 45% for $N=150$ and almost doubled (increased by 84%) for $N=300$.

B. Primitive path analysis

As mentioned earlier, the annealing algorithm developed for linear chains had to be modified for rings. The motivation for doing so may be understood from the following example: Consider a system comprised wholly of nonconcatenated rings. Such a system may develop features like the "reef knot" shown in Fig. 2. While such a feature is not, in the mathematical sense, a true knot, it is a matter of convention to refer to it by the name "reef knot." While such features could contribute to the elastic free energy of a polymer melt, their contribution may or may not be significant. In light of the inconclusive evidence for the existence of a plateau modulus in a melt of ring polymers, such features were considered to be devoid of entanglements. While such a choice is arbitrary, the evidence to choose otherwise is not compelling. Thus, all the PPs should, in principle, collapse to a point. Extending the annealing algorithm developed for linears to rings, the adjacent "end" beads 1 and N_R are immobilized, and upon annealing, one would expect the PP to collapse to a straight line segment connecting these end beads. However, certain configurations like the one shown in Fig. 2 would inadvertently introduce spurious features in the resulting PP network. The "reef knot" shown in Fig. 2 is made up of two nonconcatenated rings. If these rings are fixed at A and B and their contour lengths are reduced as annealing proceeds, it may be seen upon inspection that these two chains cannot be unraveled as long as they are fixed at A and B.

Indeed, such structures were frequently observed in a melt of pure rings with $N_R=300$, when the annealing operation was carried out by fixing beads 1 and N_R. For melts with smaller rings $N_R<50$ such knotted conformations were rare, indicating that the probability of their occurrence increases with the degree of polymerization.

To overcome the problem, the beads that were immobilized during the course of annealing were periodically varied. Thus, at every fixed interval of time ($\approx 0.1-1.0\tau_e$) a fresh pair of consecutive beads was held fixed, and the beads restrained in the preceding time interval were released. For

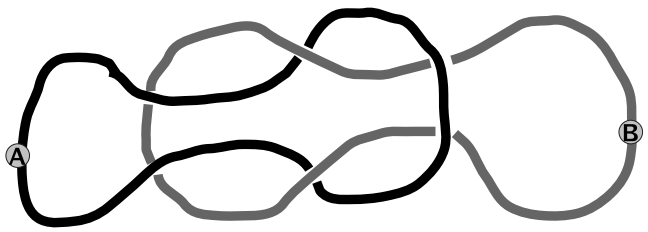

FIG. 2. Two nonconcatenated rings affixed at points A and B forming a "reef knot."

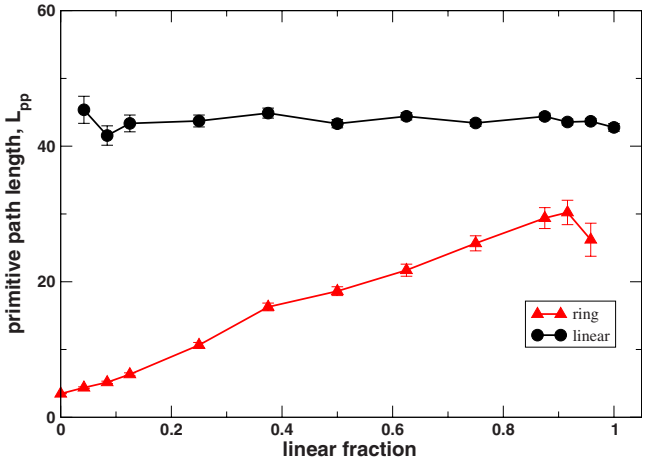

FIG. 3. (Color online) Mean primitive path length of rings (triangles) and linear chains (circles) for a blend of ring and linear molecules with $N_R=N_L=150$ at different compositions. As the fraction of linear chains ϕ_L/ϕ increases, average primitive path length of the rings increases, while average primitive path length of the linear chains remains relatively unchanged.

$\tau_{\text{anneal}}=10\tau_e$, results were insensitive to the length of the time interval for the cases considered in this study.

When this algorithm was employed on a melt of pure rings, the PPs of all the rings collapsed to the configuration shown in Fig. 7(a). The resulting PP was triangular and had three beads. The structure does not get any simpler and collapse to a straight line or a point, because in order to prevent chains from passing through each other, midpoints of bonds are not allowed to overlap in S-BFM. This is an artifact of the particular lattice model chosen and is absent in off-lattice simulations. It cannot be avoided unless the underlying lattice description is altered. However, this turns out to be inconsequential, since the resulting PP length is much smaller (on the order of 3) than the PP length of the rings as ϕ_L increases.

Figures 3 and 4 show the average PP lengths of the ring and linear species L_{ppR} and L_{ppL} as a function of ϕ_L for $N=150$ and 300, respectively. L_{ppL} was essentially independent of ϕ_L. The effect on L_{ppR} was more dramatic, and it increased approximately linearly with ϕ_L. This suggests that the PP length of a single ring molecule embedded in a sea of linear chains is comparable with L_{ppL}, especially as N increases, i.e., for large N,

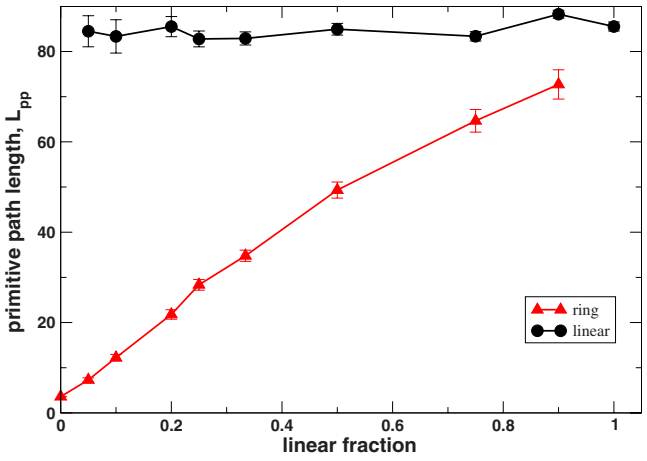

FIG. 4. (Color online) Mean primitive path length of rings (triangles) and linear chains (circles) for a blend of ring and linear molecules with $N_R=N_L=300$ at different compositions.

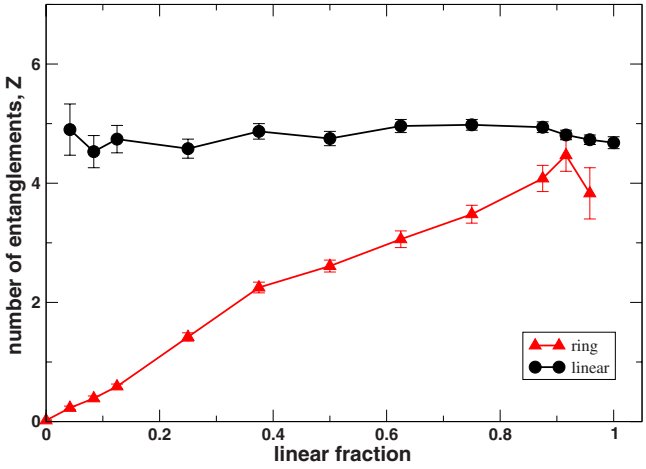

FIG. 5. (Color online) Average number of entanglements as identified by the ILD algorithm on rings (triangles) and linear chains (circles) for a blend of ring and linear molecules with $N_R=N_L=150$ at different compositions. As the fraction of linear chains ϕ_L/ϕ increases, the average number of entanglements on rings increases, while the average number of entanglements on linear chains remains relatively unchanged.

$$L_{ppR}(\phi_L) \approx \frac{\phi_L}{\phi} L_{ppL}. \tag{2}$$

The average number of entanglements computed using the ILD algorithm reinforces this description. As shown in

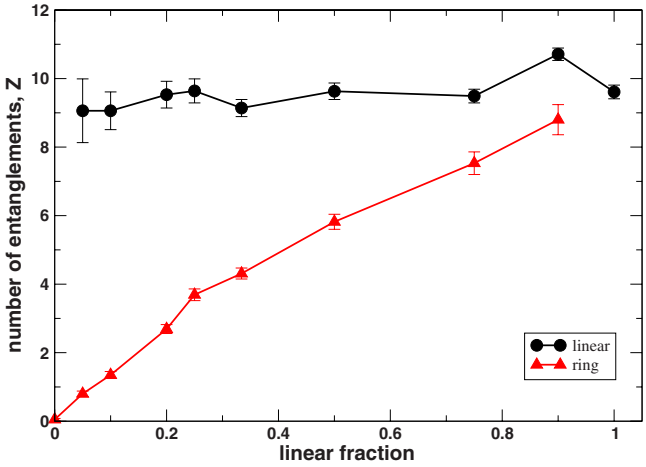

FIG. 6. (Color online) Average number of entanglements as identified by the ILD algorithm on rings (triangles) and linear chains (circles) for a blend of ring and linear molecules with $N_R=N_L=300$ at different compositions.

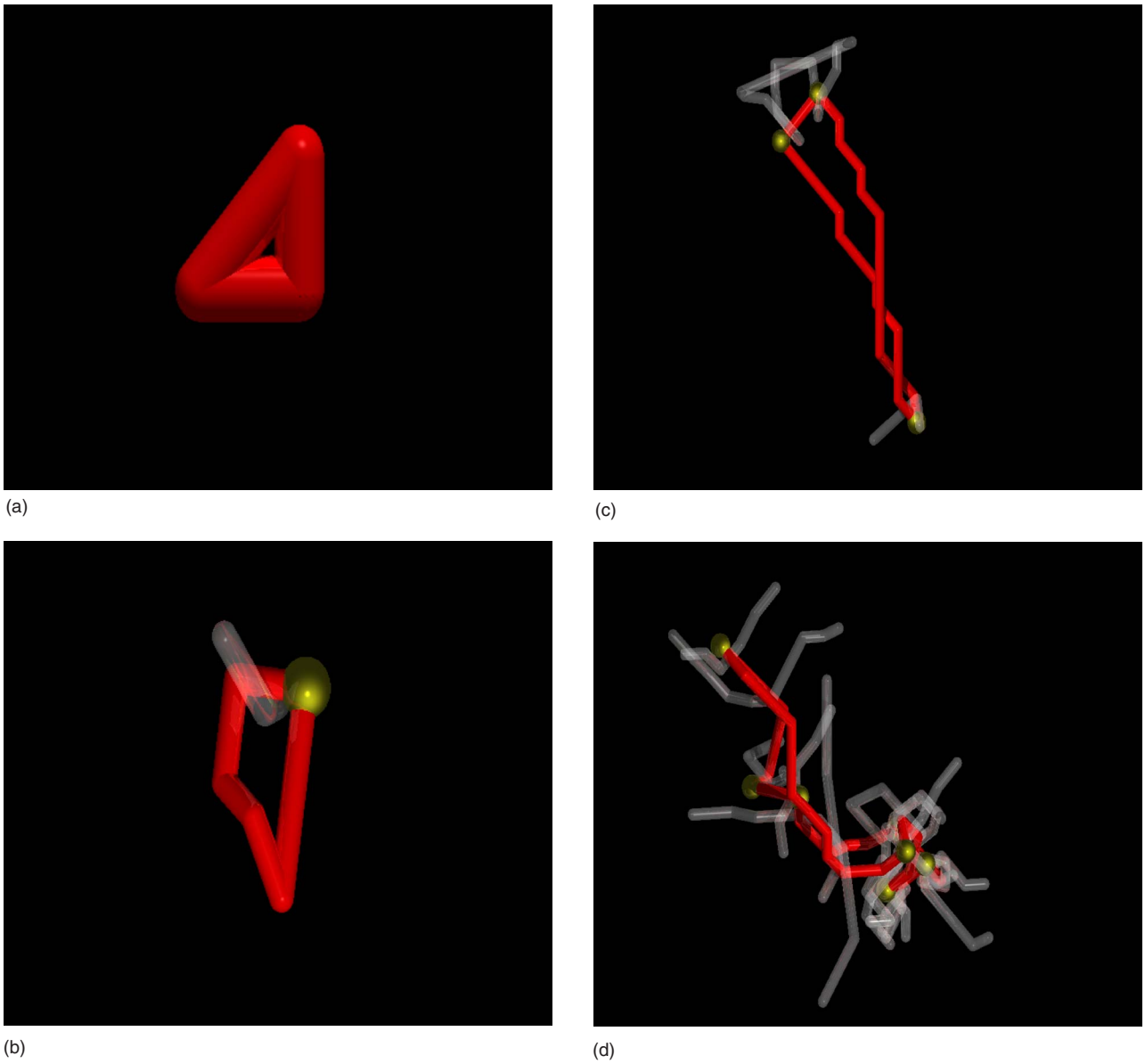

FIG. 7. (Color online) Snapshots of representative primitive paths of rings at different linear fractions for $N=300$ shows increased infiltration of ring volume by entanglements. For clarity, only a single ring molecule (solid), interacting matrix segments (transparent), and location of entanglement points as identified by the ILD algorithm are depicted. When (a) $\phi_L=0.0$, the individual rings are completely disentangled. As ϕ_L increases through (b) 0.025, (c) 0.100, and (d) 0.375, the number of entanglements increases.

Fig. 5 and 6, the average number of entanglements on a tracer ring molecule in a linear matrix approaches the average number of entanglements on the linear chains,

$$Z_R(\phi_L) \approx \frac{\phi_L}{\phi} Z_L. \tag{3}$$

It is interesting to note that for $N=150$, Eq. (3) is satisfied, while Eq. (2) does not appear to hold. Currently, we do not have a clear explanation for this observation.

IV. DISCUSSION

Figure 7 shows representative snapshots of PPs of rings when ϕ_L is varied for $N=300$. The agreement of the location of entanglement points identified by the ILD algorithm and the associated PPs of matrix chains appears to be excellent. As linear chains are introduced into a melt of rings ($\phi_L=0.025$), the PP of the rings becomes entangled and longer. For some rings, *in the presence of linear chains*, the PPs of two rings sometimes interact with each other topologically which, while not entirely unexpected, is an interesting departure from the case of pure rings where the PPs of the nonconcatenated rings do not interfere with each other. One such example is shown in Fig. 7(c), where the two entanglements at the top of the figure arise due a neighboring ring molecule, which is itself unable to shrink further. Thus, the effect of linear chains is not merely confined to simple ring-linear interactions as shown in Fig. 7(b). It is additionally mani-

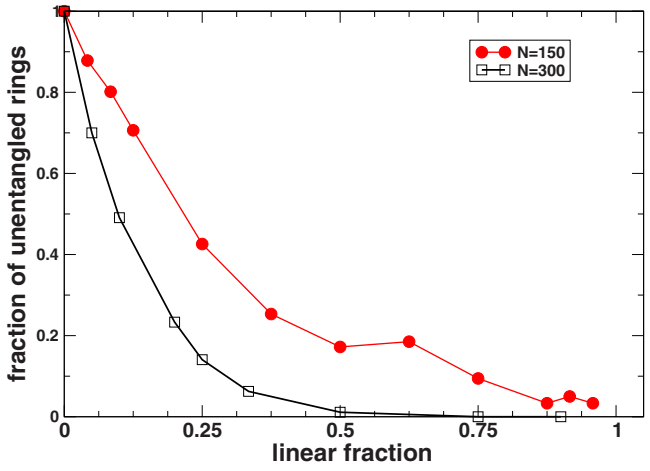

FIG. 8. (Color online) Fraction of unentangled rings decreases from unity (pure rings) to zero as the fraction of the linear chains increases. The decrease is more rapid as N increases.

fested through ring-ring interactions that are otherwise absent when $\phi_L=0$.

Threading of rings by linear chains. It was reported earlier that the introduction of small quantities of linear chains (in the limit $\phi_L \to 0$) in a melt of pure rings can cause a disproportionate increase in the zero-shear viscosity [23,24]. It was shown in Sec. III A and in a previous work [22] that rings expand in the presence of linear chains. It is conceivable that a single linear chain "threads" through several swollen ring polymers thereby curtailing their motion. Such rings can relax or diffuse only on the time scale of reptation of the linear chain.

A rough estimate for the number of rings "engaged" by a linear chain (in the limit $\phi_L \to 0$) is Z_L [24]. This assumes that each linear chain passes through a ring molecule only once and that two linear chains do not interact, and is therefore expected to overestimate the number of ring molecules that are threaded. Under these assumptions, the fraction of rings that remain unengaged, ϕ_R^u/ϕ_R, is given by

$$\frac{\phi_R^u}{\phi_R} = 1 - \frac{\phi_L Z_L}{\phi_R}. \tag{4}$$

The fraction of rings with no entanglements, ϕ_R^u/ϕ_R, was computed using the ILD algorithm for all the systems considered in Table I (see Fig. 8). For pure rings, ϕ_R^u/ϕ_R decreased from unity to zero as the fraction of the linear chains increased. The decrease was more rapid as N increased from 150 to 300. In the limit of small fraction of linear chains ($\phi_L/\phi=0.05$), the fraction of engaged rings increased from about 13% for $N=150$ to about 30% for $N=300$.

As expected, these values are lower than those predicted by Eq. (4), which estimates the fraction of engaged rings to be approximately 25% and 50% for $N=150$ and 300, respectively, at $\phi_L/\phi=0.05$. It may be pointed out that at $\phi_L/\phi=0.05$ there is some interaction between linear chains, as the crossover concentrations based on the radius of gyration are

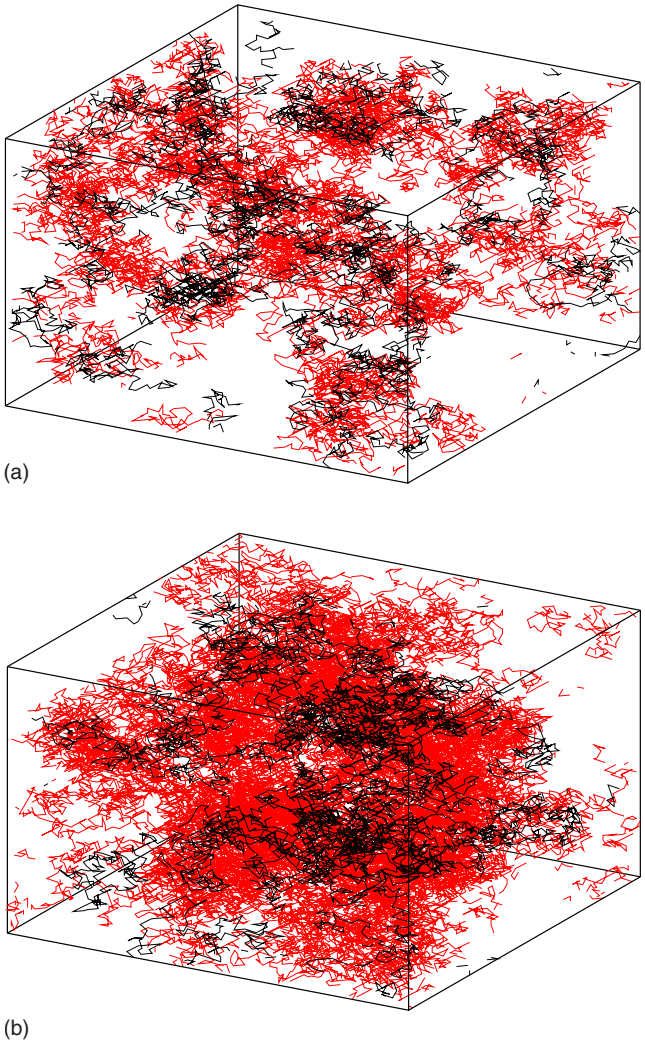

FIG. 9. (Color online) Simulation box showing only entangled polymer chains. Linears (solid black) thread through multiple rings inducing ring-ring interactions and form a percolating network that spans the entire simulation box. (a) N=150 with $\phi_L/\phi=0.042$ and (b) N=300 with $\phi_L/\phi=0.05$. Note: The periodic boundary condition causes some rings to appear as linears with small molecular weight.

approximately equal to $\phi_L/\phi=0.15$ and 0.10 for $N=150$ and $N=300$, respectively.

Nevertheless, the PP analysis indicates that a sizable fraction of ring molecules are threaded by linear chains at relatively low linear concentrations, which further increases with N. The ratio of volume occupied by engaged polymers (i.e., polymers with entanglements) to total volume of the simulation box may be estimated as

$$\frac{V_e}{V} = \frac{1}{L^3}\left(N_{pL}^e \frac{4}{3}\pi\langle R_{gL}\rangle^3 + N_{pR}^e \frac{4}{3}\pi\langle R_{gR}\rangle^3\right), \tag{5}$$

where the superscript e denotes engaged polymers.

This ratio was found to be 0.54 for $N=150$ and 1.32 for $N=300$ at the lowest nonzero concentration of linears considered in this study. This calculation is an overestimate, as

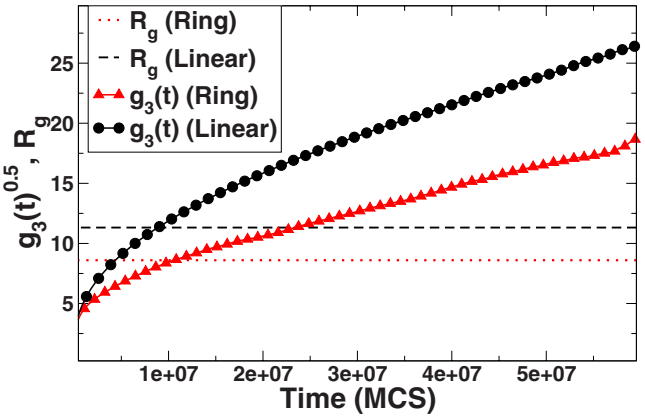

FIG. 10. (Color online) Plot of distance diffused by rings and linears as a function of time for the slowest system considered in this study, $N=300$ and $\phi_L=0.45$. Horizontal lines indicate equilibrated $\langle R_g \rangle$.

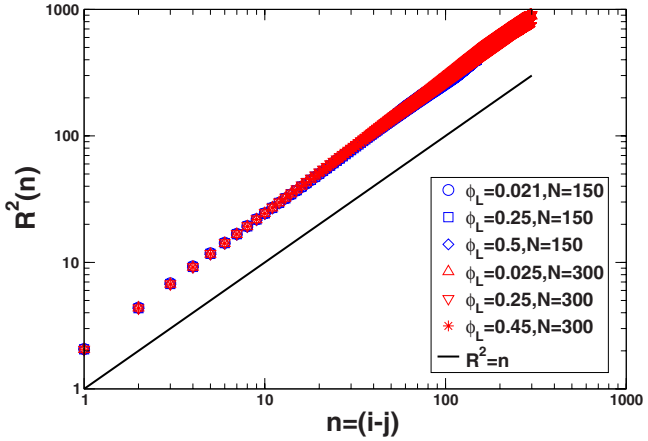

FIG. 11. (Color online) For well equilibrated linears $R^2(n) \sim n^{1.0}$, when $n \gg 1$ demonstrating the Gaussian character of the linears at all but the smallest length scales. The solid line has a slope of unity.

the volume occupied by two polymers may overlap. However, it indicates that the volume occupied by the engaged polymers may be sufficient to form a percolating network. Figure 9 shows only the engaged polymers (i.e., polymers with entanglements) for both molecular weights, again, at the lowest nonzero concentration of linears considered in this study. It may be seen that the entangled polymers form a percolating network that spans the entire simulation box, especially for $N=300$. Therefore, it may be concluded that even in the presence of a small fraction of linear chains, entanglement effects can permeate the entire system. This could be the origin of the unexpected sensitivity of the dynamics of ring-linear systems.

Finally, a qualifying word on the different interpretations of the PP of cyclic polymers is in order. For noncyclic polymers, such as linears and stars, the annealing algorithm seeks the shortest contour affixing the ends of all the polymers which obeys all topological constraints in the system [38]. When this definition is applied to unknotted and nonconcatenated rings without immobilizing any fixed set of beads, the PP is bound to reduce to a single point independent of N. This definition of PP is different from that used elsewhere [5,6], where it is assumed that rings are large enough to adopt lattice "animal" configurations and that their "trunk" may be considered a PP whose diffusive motions govern the dynamics. In the former interpretation, the length of the PP of rings remains constant ($L_{ppR} \sim 0$), and in the latter, it depends on the ring size ($L_{ppR} \sim N^{0.5}$).

Similarly, it was suggested [18] that $N_{eR} \approx 2-5N_{eL}$, where N_{eR} and N_{eL} are the number of monomers per entanglement segment for rings and linear chains, respectively. However, for long pure rings, we find that $N_{eR} \to \infty$, since both Z_R and L_{ppR} approach zero.

V. SUMMARY

An adapted version of the annealing algorithm to identify the PPs of a melt of ring polymers was presented. As expected, the PPs collapse to zero length for nonconcatenated rings, and no entanglements are observed. However, when some of the ring polymers were substituted with linear chains, the PP length increased approximately linearly with the fraction of linear chains, $L_{ppR} \sim \phi_L/\phi$. Like the radius of gyration, the PP length of a linear chain, L_{ppL} was independent of the composition of the blend. For large N, in the limit $\phi_L/\phi \to 0$, $L_{ppR} \approx L_{ppL}$. The average number of entanglements on the ring and linear chains followed an identical trend.

The PP calculations of the ring-linear blends quantify how the volume of a ring polymer is pervaded by neighboring linear and ring molecules. They show threading of rings by linears, as well as ring-ring interactions that come into play only in the presence of linear chains. It is suggested that these ring-ring interactions enable the formation of a percolating entangled network even when the linear chain fraction is too small to percolate by itself. This could help explain the extreme sensitivity of the linear viscoelasticity to the fraction of linear chains.

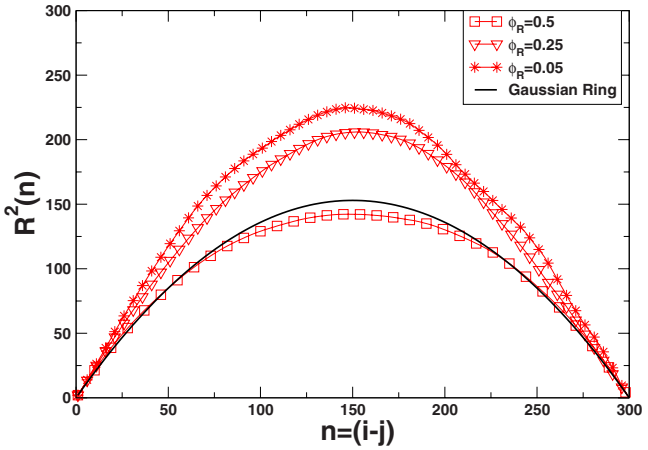

FIG. 12. (Color online) For equilibrated rings with $N=300$, the shape of the $R^2(n)$ curve is similar to that of Gaussian rings. The rings are compressed in a melt of pure rings and start to swell as the fraction of linears is increased.

ACKNOWLEDGMENTS

The authors would like to acknowledge Dr. Ashish Lele for helpful discussions. Partial support for this work was provided by Florida State University Grant No. CRC-PG-020837 and the Petroleum Research Foundation through ACS PRF Grant No. 46770-G7.

APPENDIX: EQUILIBRATION

To test whether the polymers were properly equilibrated, the mean squared distance diffused by each polymer chain (both rings and linears), $g_3(t)$, was computed for the slowest system considered in this study ($N=300$ and $\phi_L=0.45$) using:

$$g_3(t) = \langle [\mathbf{R}_{\mathrm{CM}}(t) - \mathbf{R}_{CM}(0)] \cdot [\mathbf{R}_{\mathrm{CM}}(t) - \mathbf{R}_{\mathrm{CM}}(0)] \rangle \quad \text{(A1)}$$

where $\mathbf{R}_{\mathrm{CM}}(t)$ is the vector denoting the center of mass of a particular polymer at time t. The results are shown in Fig. 10. It may be seen that in the time taken for both p_R and p_L to drop below 0.1 (6×10^7 MCS), the rings and linears have on average diffused a distance approximately equal to their radius of gyration, thereby suggesting that the systems are indeed well equilibrated.

Further, the distance between internal beads of equilibrated polymers was examined. For a given polymer of N beads, let $\mathbf{R}(i)$ and $\mathbf{R}(j)$ be the coordinates of beads i and j, respectively. Further, let $n=(i-j)$ and,

$$R^2(n) = \langle [\mathbf{R}(i) - \mathbf{R}(j)] \cdot [\mathbf{R}(i) - \mathbf{R}(j)] \rangle. \quad \text{(A2)}$$

For a given system, the ensemble-averaged $R^2(n)$ was computed over all possible pairs of beads i and j such that $i-j=n$.

A plot of the resulting average $R^2(n)$ versus n of the linears for the different N of a few representative systems considered is shown in Fig. 11. For $n \gg 1$, $R^2(n) \sim n^{1.0}$ demonstrating that the linears are well equilibrated.

For Gaussian rings, $R^2(n)$ as a function of n is given by [39]

$$R^2(n) = b^2 n \left(1 - \frac{n}{N}\right), \quad \text{(A3)}$$

where the mean bond length $b=1.428$ [28]. Figure 12 shows average $R^2(n)$ versus n for a few representative ring systems at $N=300$. It may be seen that rings are compressed in a melt of pure rings and swell as the fraction of linears increases. The plot of $R^2(n)$ versus n did not change significantly after both $p_L(t)$ and $p_R(t)$ dropped below 0.1, even after the polymers had diffused multiple radii of gyration. This suggests that all systems considered are indeed well equilibrated at all length scales.

[1] R. C. Ball and T. C. B. Mcleish, Macromolecules **22**, 1911 (1989).
[2] P. G. de Gennes, *Scaling Concepts in Polymer Physics*, 1st ed. (Cornell University Press, Ithaca, 1979).
[3] M. Doi and S. F. Edwards, *The Theory of Polymer Dynamics* (Clarendon Press, Oxford, 1986).
[4] M. E. Cates and J. M. Deutsch, J. Phys. (Paris) **47**, 2121 (1986).
[5] B. V. S. Iyer, A. K. Lele, and V. A. Juvekar, Phys. Rev. E **74**, 021805 (2006).
[6] S. P. Obukhov, M. Rubinstein, and T. Duke, Phys. Rev. Lett. **73**, 1263 (1994).
[7] M. Rubinstein, Phys. Rev. Lett. **57**, 3023 (1986).
[8] G. B. McKenna, G. Hadziioannou, P. Lutz, G. Hild, C. Strazielle, C. Straupe, P. Rempp, and A. J. Kovacs, Macromolecules **20**, 498 (1987).
[9] G. B. McKenna, B. J. Hostetter, N. Hadjichristidis, L. J. Fetters, and D. J. Plazek, Macromolecules **22**, 1834 (1989).
[10] J. Roovers, Macromolecules **18**, 1359 (1985).
[11] J. Roovers and P. M. Toporowski J. Polym. Sci., Part B: Polym. Phys. **26**, 1251 (1988).
[12] C. W. Bielawski, D. Benitez, and R. H. Grubbs, Science **297**, 2041 (2002).
[13] S. Brown, T. Lenczycki, and G. Szamel, Phys. Rev. E **63**, 052801 (2001).
[14] S. Brown and G. Szamel, J. Chem. Phys. **109**, 6184 (1998).
[15] S. Brown and G. Szamel, J. Chem. Phys. **108**, 4705 (1998).
[16] K. Hur, R. G. Winkler, and D. Y. Yoon, Macromolecules **39**, 3975 (2006).
[17] M. Müller, J. P. Wittmer, and J. L. Barrat, Europhys. Lett. **52**, 406 (2000).
[18] M. Müller, J. P. Wittmer, and M. E. Cates, Phys. Rev. E **53**, 5063 (1996).
[19] M. Müller, J. P. Wittmer, and M. E. Cates, Phys. Rev. E **61**, 4078 (2000).
[20] R. Ozisik, E. D. von Meerwall, and W. L. Mattice, Polymer **43**, 629 (2002).
[21] S. Geyler and T. Pakula, Makromol. Chem., Rapid Commun. **9**, 617 (1988).
[22] B. V. S. Iyer, A. K. Lele, and S. Shanbhag, Macromolecules **40**, 5995 (2007).
[23] G. B. McKenna and D. J. Plazek, Polym. Commun. **27**, 304 (1986).
[24] M. Kapnistos, M. Lang, M. Rubinstein, J. Roovers, T. Chang, and D. Vlassopoulos, Society of Rheology Annual Meeting, 2006.
[25] R. M. Robertson and D. E. Smith, Macromolecules **40**, 3373 (2007).
[26] R. M. Robertson and D. E. Smith, Proc. Natl. Acad. Sci. U.S.A. **104**, 4824 (2007).
[27] J. S. Shaffer, J. Chem. Phys. **101**, 4205 (1994).
[28] S. Shanbhag and R. G. Larson, Phys. Rev. Lett. **94**(7), 076001 (2005).
[29] S. Brown and G. Szamel, Macromol. Theory Simul. **9**, 14 (2000).
[30] R. Everaers, S. K. Sukumaran, G. S. Grest, C. Svaneborg, A. Sivasubramanian, and K. Kremer, Science **303**, 823 (2004).
[31] R. G. Larson, Q. Zhou, S. Shanbhag, and S. J. Park, AIChE J.

53, 542 (2007).
[32] S. Shanbhag, S. J. Park, Q. Zhou, and R. G. Larson, Mol. Phys. **105**, 249 (2007).
[33] S. Shanbhag and M. Kroger, Macromolecules **40**, 2897 (2007).
[34] S. Shanbhag and R. G. Larson, Macromolecules **39**, 2413 (2006).
[35] J. S. Shaffer, J. Chem. Phys. **103**, 761 (1995).
[36] M. Kröger, Comput. Phys. Commun. **168**, 209 (2005).
[37] C. Tzoumanekas and D. N. Theodorou, Macromolecules **39**, 4592 (2006).
[38] S. F. Edwards, Proc. Phys. Soc. **91**, 513 (1967).
[39] B. H. Zimm and W. H. Stockmayer, J. Chem. Phys. **17**, 1301 (1949).